Fermi-Level Alignment at Metal-Carbon Nanotube Interfaces: Application to Scanning Tunneling Spectroscopy

Yongqiang Xue* and Supriyo Datta
School of Electrical and Computer Engineering, Purdue University, West Lafayette, Indiana 47907
(Received 5 August 1999)

At any metal-carbon nanotube interface there is charge transfer and the induced interfacial field determines the position of the carbon nanotube band structure relative to the metal Fermi level. In the case of a single-wall carbon nanotube supported on a gold substrate, we show that the charge transfers induce a local electrostatic potential perturbation which gives rise to the observed Fermi-level shift in scanning tunneling spectroscopy measurements. We also discuss the relevance of this study to recent experiments on carbon nanotube transistors and argue that the Fermi-level alignment will be different for carbon nanotube transistors with low resistance and high resistance contacts.

PACS numbers: 73.61.Wp, 61.16.Ch, 73.20.–r, 73.50.–h

The discovery of carbon nanotube opens up a new artificial laboratory in which one-dimensional transport can be investigated [1], similar to the semiconductor quantum wire [2]. However, the study of transport in carbon nanotube has been complicated by the difficulty of making low resistance contacts to the measuring electrodes. The high resistances reported in various two- and three-terminal measurements [3] have led Tersoff [4] (and also the present authors [5]) to suggest that wave vector conservation at the metal-carbon nanotube contact may play an important role in explaining the high contact resistance. In this paper we address a different question: How does the Fermi level in the metallic contact align with the energy levels of the nanotube? The answer to this question is very important in interpreting the transport measurements. Depending on the contact geometry, transport can occur in the direction parallel to the nanotube axis, in the case of nanotube field-effect-transistor (FET) [3,6], or perpendicular to it, in the case of the scanning tunneling spectroscopy (STS) measurement [7]. In the STS measurement, the Fermi level is found to have shifted to the valence band edge of the semiconducting nanotube [7], which is then used to explain the operation of the nanotube FETs with high resistance contacts [3], where the measured two-terminal resistance for metallic nanotube is $\sim 1\ \mathrm{M}\Omega$. However, low temperature transport measurements using low resistance contacts [6] (where the contact resistance is of the order of resistance quantum) indicate that the Fermi level is located between the valence and conduction band of the semiconducting nanotube, instead of being pinned to the valence band edge. This conflict raises the important question of whether the Fermi-level positioning may depend on the contact geometry and/or the interface coupling.

In this paper we present a theory of the scanning tunneling spectroscopy of a single-wall carbon nanotube (SWNT) supported on the Au(111) substrate. The main results of our work are the following: (i) The work function difference between the gold substrate and the nanotube leads to charge transfers across the interface, which induces a local electrostatic potential perturbation on the nanotube side giving rise to the observed Fermi-level shift in the STS measurement. (ii) For nanotube transistors, the atomic-scale potential perturbation at the interface is not important *if the coupling between the metal and the nanotube is strong*. The metal-induced gap states (MIGS) model provides a good starting point for determining the Fermi-level position. (iii) A proper theory of STS should take the tip electronic structure into account.

For an ordinary metal-semiconductor interface, the MIGS model provides a conceptually simple way of understanding the band lineup problem which predicts that the metal Fermi-level E_F should align with the "charge neutrality level" (which can be taken as the energy where the gap states cross over from valence- to conduction-type character) in the semiconductor [8]. This elegant idea has been applied with impressive success by Tersoff to various metal-semiconductor junctions and semiconductor heterojunctions, which greatly simplifies the band lineup problem and gives quantitatively accurate prediction of the Schottky barrier height in many cases [8,9]. The success of this model relies on the fact that there exists a continuum of gap states around E_F at the semiconductor side of the metal-semiconductor interface due to the tails of the metal wave function decaying into the semiconductor, which can have significant amplitude over a few atomic layers near the interface [10]. Any deviation from local charge neutrality in the interface region will result in metallic screening by the MIGS.

However, this is not true for the interface formed when a SWNT is deposited onto the gold substrate. Since the coupling to the substrate is weak and the metal wave function decays across a significant van der Waals separation [4,11], the MIGS will provide only relatively weak screening. When the conductance spectrum is measured using a scanning tunneling microscope (STM),

 0031-9007/99/83(23)/4844(4)$15.00

transport occurs perpendicular to the nanotube axis and the characteristic length scale is the diameter of the SWNT which is on the scale of nanometers [7] and can be comparable to the range of the interfacial perturbation. The detailed potential variations in this dimension will be important in determining the STS current-voltage characteristics, similar to the case of molecular adsorbates on metal surfaces [12]. Figure 1 illustrates schematically the local electrostatic potential profile at the substrate-nanotube-tip heterojunction. If the charge distributions on both sides do not change when interface is formed, then the vacuum levels line up [8]. However, due to the difference of work functions [3,7] [as shown in Fig. 1(b)], electrons will transfer from the SWNT to the gold substrate and the resulting electrostatic potential profile $\delta\phi$ should be determined self-consistently (since the perturbation due to the tip is much weaker, we neglect its effect when treating the substrate-SWNT interface).

We assume an ideal substrate-SWNT interface and study the interface electronic structure using the π-electron tight-binding (TB) model of the SWNT [13]. In this model, the band structure of SWNTs is symmetric with respect to the position of the on-site π orbital energy. We take the Fermi level of the gold as the energy reference, then the initial π orbital energy at each carbon atom of the SWNT is $W_m - W_{\rm nt} = 0.8$ (eV). The

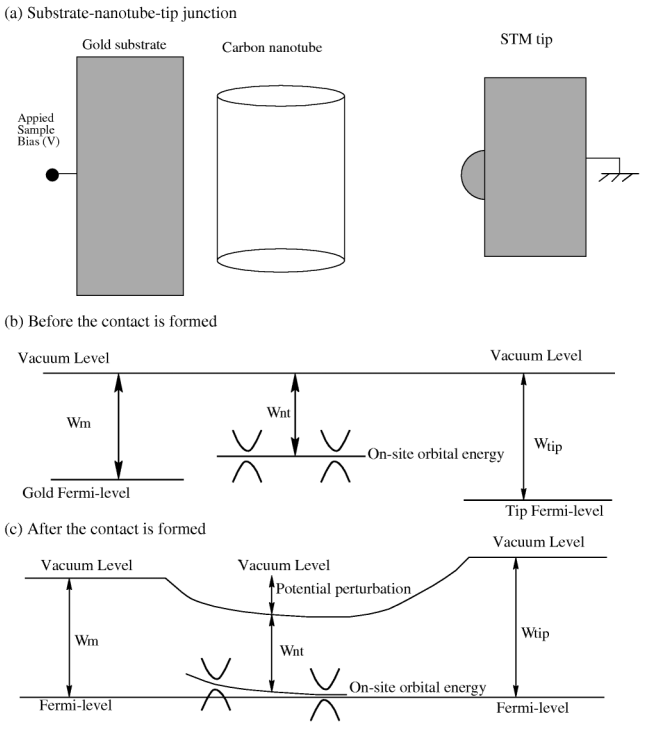

FIG. 1. Illustration of the formation of a substrate-SWNT contact. We show only a semiconducting SWNT here. The work functions of the gold, the SWNT, and the platinum tip are $W_m = 5.3$ (eV), $W_{\rm nt} = 4.5$ (eV), and $W_{\rm tip} = 5.7$ (eV), respectively. (c) shows our picture of the interface Fermi-level positioning.

final on-site π orbital energy is the superposition of this initial value and the change in the electrostatic potential $\delta\phi$ which changes as one moves away from the gold substrate [Fig. 1(c)]. For the gold substrate we use the TB parameters of Papaconstantopoulos [14]. For the coupling between the SWNT and the gold surface, we use the values obtained from the extended Hückel theory [15]. Only the carbon atoms closest to the gold surface are assumed to be coupled [16].

Since the SWNT has periodic symmetry along its axis, only one unit cell needs to be considered. We use the Green's function method to calculate the electron population of each carbon atom from the expression: $n_i = -\frac{2}{\pi}\,\mathrm{Im}\{\int_{-\infty}^{E_F} G_{i,i}(E)\,dE\}$, where $G(E)$ is the projection of the Green's function onto one unit cell of the SWNT and $G_{i,i}$ is the ith diagonal matrix element corresponding to atom i in the unit cell. $G(E)$ is calculated by reducing the Hamiltonian of the whole interface into an effective one in which the interactions between the given unit cell and the rest of the interface system are incorporated into the corresponding self-energy operators using the same method as described in Chap. 3 of Datta [2]. Within the tight-binding theory, self-consistency is achieved by adjusting the diagonal elements of the Hamiltonian and imposing Hartree consistency between the potential perturbation $\delta\phi_i$ and the charge perturbation δn_i using the self-consistent scheme similar to that developed by Flores and co-workers [17] and also Harrison [18] (for details see Ref. [19]).

Figures 2(a) and 2(b) and Figs. 3(a) and 3(b) show the results for (10,10) and (16,0) SWNTs with diameters of 1.35 and 1.25 (nm), respectively, close to those measured in Ref. [7]. The substrate-SWNT distance is 3.2 (Å) [20]. We have also studied (15,0) and (14,0) SWNTs. All nanotubes show similar behavior. We believe similar conclusions can be reached for chiral nanotubes since the electronic structure of SWNTs depends only on their metallicity and diameter, not on chirality [21]. The similarity between the metallic and the semiconducting nanotube shown here can be understood from the work of Benedict *et al.* [22], who show that the dielectric response of SWNTs in the direction perpendicular to the axis does not depend on the metallicity, only on the diameter.

Since the π orbital energy coincides with the position of the Fermi level (midgap level) of the isolated metallic (semiconducting) SWNT, then the Fermi-level shift in the STS measurement should correspond to the on-site π orbital energy of the carbon atom closest to the STM tip *if only this atom is coupled to the tip*. However, considering the cylindrical shape of the SWNT, more carbon atoms could be coupled to the tip and the Fermi-level shift then corresponds to the average value of the on-site orbital energies of the carbon atoms within the coupling range. From the plotted values of Fig. 2 and Fig. 3, we then expect Fermi-level shifts of $\sim$0.2 (eV) for both nanotubes, close to the measured

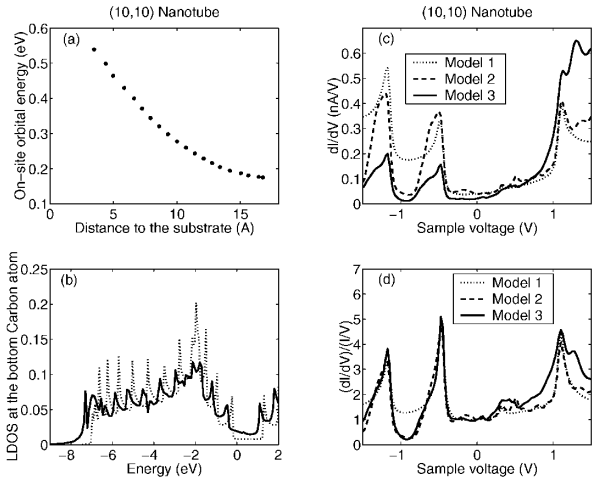

FIG. 2. Calculated results for (10,10) nanotube. (b) shows the LDOS at the carbon atom closest to the substrate in units of (states/eV)/atom; the dotted line is that of the isolated SWNT horizontally shifted by the corresponding potential perturbation $\delta\phi_i$. (c) and (d) show the calculated STS dI/dV-V and $d\ln I/d\ln V$-V curves. Model 1: tip modeled as having a constant density of states $\rho_{\rm tip}$; model 2: tip modeled as a semi-infinite Pt(111) crystal; model 3: tip modeled as a Pt atom adsorbed on the surface of the semi-infinite Pt(111) crystal.

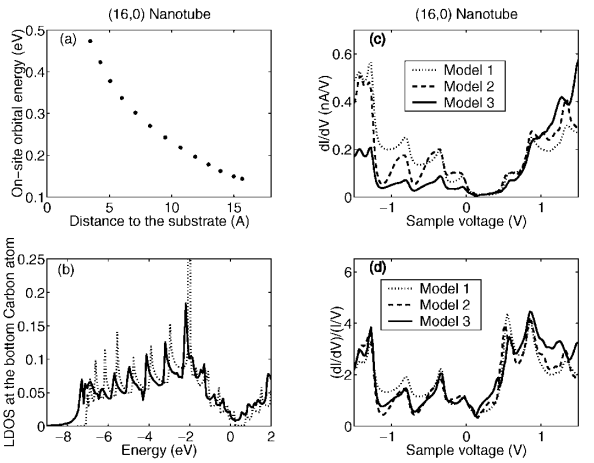

FIG. 3. Calculated results for (16,0) nanotube, otherwise the same as Fig. 2.

values [7]. The peak structures in the local density of states (LDOS) of the bottom carbon atom (closest to the gold substrate) corresponding to the Van Hove singularities are broadened due to the hybridization with the gold surface atomic orbitals. Their positions also change, which can be understood from the bonding-antibonding splitting resulting from the hybridization of the nanotube molecular orbitals and the gold orbitals. Also notable is the enhancement of the density of states in the gap at the expense of the valence band, reminding us of the Levinson theorem which states the total number of states should be conserved in the presence of perturbation, be it due to impurity or due to surface [23]. In contrast, the perturbation of the LDOS at the carbon atom furthest to the substrate is much weaker. The calculated charge transfer per atom is small and mainly localized on the carbon atoms close to the gold surface, in agreement with recent *ab initio* calculations [24].

Applications to the scanning tunneling spectroscopy.—The differential conductance dI/dV (or the normalized one $d\ln I/d\ln V$) obtained from the STS measurement is often interpreted as to reflect the local density of states of the sample, based on the *s*-wave model of the tip [25]. However, first-principles calculations have shown this model to be inadequate for tips made from transition metals, where small clusters tend to form at the tip surface giving rise to localized *d*-type tip states [26]. As a result, the tip electronic structure can have profound effects on the interpretation of the STS measurement [12,26].

The STS current-voltage characteristics can be calculated using the standard technique of scattering theory [2,12]. Here we have taken a simpler approach instead, aiming only to illustrate how the tip electronic structure may affects the interpretation of the STS measurement. Since the coupling across the SWNT-tip interface is weak, the tunneling Hamiltonian theory may be invoked to write the current crudely as

$$I \propto \int_0^{eV} \rho_{\rm nt}(E)\rho_{\rm tip}(E - eV)\, dE\,, \qquad (1)$$

where $\rho_{\rm nt}$ and $\rho_{\rm tip}$ are the density of states of the SWNT and the tip, respectively. The differential conductance thus obtained then reflects the convolution of the density of states of the SWNT and the tip. If $\rho_{\rm tip}$ is constant within the range of the integral, we recover the usual expression $dI/dV \propto \rho_{\rm nt}$. Note $\rho_{\rm nt}$ is calculated taking the on-site perturbations and the coupling to the gold substrate into account (we use the LDOS of the carbon atom closest to the tip here). We have used two models for the tip: (i) as a semi-infinite Pt(111) crystal; (ii) as a Pt atom adsorbed on the surface of the semi-infinite Pt(111) crystal [12]. The results are shown in Figs. 2(c) and 2(d) and Figs. 3(c) and 3(d) along with that obtained from Eq. (1) assuming constant $\rho_{\rm tip}$. As can be seen from the plots, additional fine structures are introduced between the peak structures of $\rho_{\rm nt}$ when we take into account the electronic structure of the tip.

Discussions and conclusions.—With the advancement of new techniques for making electric contact to the SWNT [6,27], low resistance contacts with two-terminal conductance close to the conductance quantum have been obtained [28]. Current-voltage characteristics measured at low temperature using these new techniques show that the Fermi level is located in the gap of the semiconducting SWNT. In these experiments, SWNTs are grown from the patterned catalyst islands on the silicon wafer; Au/Ti contact pads are then placed on the catalyst islands fully covering the islands and extending over their edge [6].

Since the SWNTs thus grown are mostly capped [27], the coupling between the SWNTs and the electrode is presumably similar to that of fullerene where it is well known that fullerene forms a strong chemical bond with the noble and transition metal surfaces (see Dresselhaus *et al.* [29]). The large contact area between the SWNTs and the metal will make the coupling across the interface even stronger which then allows the metal wave functions to penetrate deep into the nanotube side. Therefore, we expect that the dominant contribution to the barrier height is from the metallic screening by MIGS, which tends to line up the metal Fermi level with the charge neutrality level of the SWNT. Since the band structure of the SWNT is exactly symmetric within the π-electron model, the charge neutrality level will be at the mid-gap, although it can be different when a more accurate model of electronic structure is used. Our emphasis here is not to give a quantitative estimate of the barrier height, but rather to show that the MIGS model provides the conceptual base of understanding in the limit of strong interface coupling. The situation gets complicated for measurements using high resistance contacts, where the SWNT is side contacted [3] and the coupling across the interface is weak [4,11]. In this case, the MIGS model of Schottky barrier is no longer applicable. The interface defects and bending of SWNT at the edge of the contact can induce localized states at the interface region [11] which will accommodate additional charges and affect the formation of Schottky barrier [9]. Therefore, we expect that the final Fermi-level position depends on the detailed contact condition and *may or may not be located at the valence band edge*. We believe that a detailed *ab initio* analysis is needed to clarify the various mechanisms involved.

This work is jointly supported by NSF and ARO through Grant No. 9708107-DMR. We are indebted to M. P. Anantram for drawing our attention to this important topic.

*Email address: yxue@ecn.purdue.edu

[1] C. Dekker, Phys. Today **52**, No. 5, 22 (1999).
[2] S. Datta, *Electron Transport in Mesoscopic Systems* (Cambridge University Press, Cambridge, England, 1995).
[3] S. J. Tans, A. R. M. Verschueren, and C. Dekker, Nature (London) **393**, 49 (1998); R. Martel *et al.*, Appl. Phys. Lett. **73**, 2447 (1998).
[4] J. Tersoff, Appl. Phys. Lett. **74**, 2122 (1999).
[5] M. P. Anantram, S. Datta, and Y. Xue, cond-mat/9907357.
[6] H. T. Soh *et al.*, Appl. Phys. Lett. **75**, 627 (1999).
[7] J. W. G. Wildöer *et al.*, Nature (London) **391**, 59 (1998).
[8] J. Tersoff, Phys. Rev. Lett. **52**, 465 (1984); Phys. Rev. B **30**, 4874 (1984); **32**, 6968 (1985); J. Tersoff, in *Heterojunction Band Discontinuities: Physics and Device Applications*, edited by F. Capasso and G. Margaritondo (North-Holland, Amsterdam, 1987).
[9] For review of recent works, see W. Mönch, Rep. Prog. Phys. **53**, 221 (1990); G. Margaritondo, Rep. Prog. Phys. **62**, 765 (1999).
[10] V. Heine, Phys. Rev. **138**, A1689 (1965); C. Tejedor, F. Flores, and E. Louis, J. Phys. C **10**, 2163 (1977).
[11] A. Rochefort *et al.*, cond-mat/9904083.
[12] Y. Xue *et al.*, Phys. Rev. B **59**, 7852 (1999), and references therein.
[13] R. Saito, G. Dresselhaus, and M. S. Dresselhaus, *Physical Properties of Carbon Nanotubes* (Imperial College Press, London, 1998).
[14] D. A. Papaconstantopoulos, *Handbook of the Band Structure of Elemental Solids* (Plenum Press, New York, 1986).
[15] R. Hoffmann, J. Chem. Phys. **39**, 1937 (1963).
[16] This should give a reasonable estimate of the interface coupling since the exact contact geometry is not known. We have checked that our results are not sensitive to small changes in the coupling parameters.
[17] F. Guinea, J. Sanchez-Dehesa, and F. Flores, J. Phys. C **16**, 6499 (1983); J. C. Durán *et al.*, Phys. Rev. B **36**, 5920 (1987).
[18] W. A. Harrison and J. E. Klepeis, Phys. Rev. B **37**, 864 (1988).
[19] Y. Xue and S. Datta (unpublished).
[20] At this distance, the coupling across the interface is weaker than the bulk correspondents. This is appropriate since the coupling between the SWNT and the substrate is not strong chemical bonding. See T. Hertel, R. Martel, and Ph. Avouris, J. Phys. Chem. B **102**, 910 (1998).
[21] J. W. Mintmire and C. T. White, Phys. Rev. Lett. **81**, 2506 (1998).
[22] L. X. Benedict, S. G. Louie, and M. L. Cohen, Phys. Rev. B **52**, 8541 (1995).
[23] J. A. Appelbaum and D. R. Hamann, Phys. Rev. B **10**, 4973 (1974); R. Rennie, Adv. Phys. **26**, 285 (1977).
[24] A. Rubio *et al.*, Phys. Rev. Lett. **82**, 3520 (1999).
[25] J. Tersoff and D. R. Hamann, Phys. Rev. B **31**, 805 (1985); N. D. Lang, *ibid.* **34**, 5947 (1986).
[26] *Scanning Tunneling Microscopy III*, edited by R. Wiesendanger and H.-J. Güntherodt (Springer-Verlag, Berlin, 1996), 2nd ed.
[27] J. Kong *et al.*, Nature (London) **395**, 878 (1998).
[28] Low resistance contact has also been obtained for multiwall carbon nanotube. See P. J. de Pablo *et al.*, Appl. Phys. Lett. **74**, 323 (1999).
[29] M. S. Dresselhaus, G. Dresselhaus, and P. C. Eklund, *Science of Fullerenes and Carbon Nanotubes* (Academic Press, San Diego, 1996), Chap. 17.